Rapid Communications

Synthesis of Ni_2H_3 at high temperatures and pressures

Jack Binns,[1] Mary-Ellen Donnelly,[1] Mengnan Wang,[1] Andreas Hermann,[2] Eugene Gregoryanz,[1,2] Philip Dalladay-Simpson,[1] and Ross T. Howie[1,*]

[1]*Center for High Pressure Science and Technology Advanced Research (HPSTAR), Shanghai 201203, China*

[2]*Centre for Science at Extreme Conditions and The School of Physics and Astronomy, The University of Edinburgh, Peter Guthrie Tait Road, Edinburgh EH9 3FD, United Kingdom*

(Received 21 August 2018; published 11 October 2018)

In situ high-pressure high-temperature synchrotron x-ray diffraction studies of the nickel-hydrogen system reveals the synthesis of a nickel polyhydride, Ni_2H_3. We observe the formation of NiH at pressures above 1 GPa, which remains stable to 52 GPa at room temperature. Laser heating to above 1000 K at this pressure initiates a transition to a phase which we determine as Ni_2H_3, crystallizing in a body-centered monoclinic unit cell. The Ni_2H_3 phase was observed to convert back to NiH below 25 GPa, and upon further decompression to atmospheric conditions, NiH slowly releases hydrogen with time.

DOI: 10.1103/PhysRevB.98.140101

The high-pressure synthesis and behavior of metal hydrides is an intensively studied topic of research due to the possibility of utilizing such materials for hydrogen storage purposes, and achieving predicted high-temperature superconducting states [1–3]. With the current consensus that reaching a metallic state of hydrogen remains outwith today's capabilities of diamond-anvil cell (DAC) experiments, research interests have shifted to hydrogen-dominant metallic alloys, which have also been predicted to exhibit exotic properties, such as high-temperature superconductivity [4–9]. To date the formation of hydrogen-bearing species has been theoretically explored for the majority of elements in the periodic table and recently, polyhydrides of first-row transition metals have been synthesized at high pressures [10–12]. However, there remains a gulf between the number of systems explored at pressures above 50 GPa and the extensive predictions in the literature.

The nickel-metal-hydride system has been extensively studied due to its importance as an alternative to Li-ion batteries [14]. As such, the majority of studies at pressure have been generally limited to conditions achievable by industry. Nickel has long been known to form a primary solid solution (γ_1-NiH_x with $x \approx 0.01$) near ambient conditions formed by the absorption of atomic H into the Ni lattice [15,16]. As pressure is increased above 1.25 GPa and x approaches 1, Ni adopts a face-centered-cubic structure (γ_2-NiH) with $a = 3.731$ Å (an expansion of the pure Ni fcc structure with $a = 3.5238$ Å) with H atoms occupying the octahedral sites [15,17,18]. The effects of pressure and hydrogenation on the magnetism of NiH have recently been explored through both experimental and theoretical methods [2,19,20]. However, no predictions of nickel polyhydride species have been reported to date.

Here we report, through a combination of x-ray diffraction experiments and density functional theory (DFT) calculations, the synthesis and pressure-dependent behavior of a nickel polyhydride, Ni_2H_3. This compound can be synthesized at pressures exceeding 52 GPa, and is stable on decompression to 21 GPa, below which it decomposes to the known monohydride, γ_2-NiH. Quenching the sample to atmospheric conditions, we find that γ_2-NiH slowly releases molecular hydrogen over a period of 30 min as it decomposes to its constituent elements.

High-purity nickel powder (99.8%, 1.6 μm particle size) was loaded into DACs in an inert atomosphere, together with gold and/or ruby as a pressure marker and subsequently gas loaded with research-grade hydrogen gas (99.9999%) at 0.2 GPa [21,22]. Loading of hydrogen was confirmed by the observation of the hydrogen vibrational mode using a custom-built microfocused Raman system [6]. Rhenium gaskets were used to form the sample chamber in all experimental runs; diamond-anvil culets ranged from 200 to 300 μm, with sample sizes ranging between 50 and 125 μm once hydrogen was in the solid state. Angle-dispersive x-ray diffraction patterns were recorded on a fast image-plate detector with synchrotron radiation ($\lambda = 0.4131$ Å, 30 keV) at the BL10XU beamline, SPring-8, Japan [23]. Two-dimensional image-plate data were integrated with DIOPTAS to yield intensity vs 2θ plots [24]. Diffraction patterns were indexed with CONOGRAPH; Le Bail and Rietveld refinement was carried out in JANA2006 [25–28]. Total energy calculations were carried out within the framework of DFT in conjunction with the projector-augmented wave method and a plane wave basis, as implemented in the VASP code [29,30]. We used the optB88vdw exchange-correlation functional [31,32] and included the Ni $3p$, $4s$, and $3d$ electrons in the valence space. Pure hydrogen phase I was modeled in an eight-molecule cell of $P6_3/m$ symmetry. The plane wave cutoff energy was 800 eV and Brillouin zone sampling was done on regular k-point grids with separations of 0.025 $Å^{-1}$.

After sample loading we observe the fcc structure of a primary solid solution γ_1-NiH_x [$a = 3.5223(2)$ Å at 0.6 GPa]. On further compression above 1.0(5) GPa, the sample

*ross.howie@hpstar.ac.cn

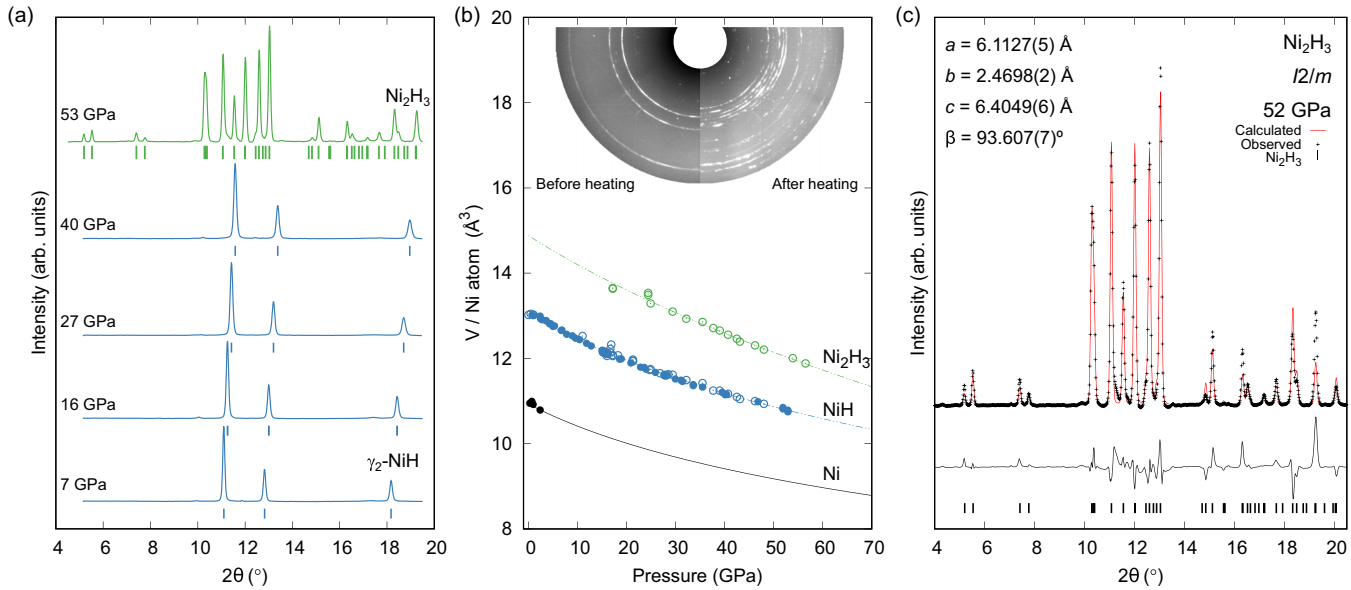

FIG. 1. (a) High-pressure x-ray diffraction patterns ($\lambda = 0.4131$ Å) showing the synthesis of Ni_2H_3 by laser heating above 50 GPa. Tick marks indicate the positions of Bragg reflections from the noted phases. (b) Atomic volume as a function of pressure for Ni (black), γ_2-NiH (blue), and Ni_2H_3 (green). Fitted equations of state are shown with dashed lines; the equation of state of Ni is shown with a solid line [13]. Closed (open) symbols correspond to data collected on (de)compression. Inset shows raw image plates before and after laser heating showing the clear formation of textured rings due to Ni_2H_3. (c) Representative Rietveld refinement of Ni_2H_3 data at 52 GPa with Ni atoms at Ni1[0.7101(6), 0, 0.0640(6)] and Ni2[0.0671(5), 0, 0.2439(6)], $wR_p = 1.94\%$, $wR_{all} = 14.19\%$.

transforms to the stoichiometric γ_2-NiH phase indicated by the appearance of new diffraction peaks that could be indexed with an expanded fcc lattice, $a = 3.7329(1)$ Å. This observation is in good agreement with previous measurements [16,19,33]. Neutron diffraction has shown the H atoms to occupy the larger octahedral vacancies in this phase, in a similar fashion to CoH and other transition-metal hydrides [10,17,34,35]. In the absence of heating, this structure remains stable on compression to at least 52 GPa, which is in good agreement with theoretical predictions [20].

In situ laser heating under compressed hydrogen has been successful in synthesizing new transition-metal compounds, particularly polyhydrides of Fe, Cr, and Co [10–12,36,37] and was applied here to explore the possibility of synthesizing nickel polyhydride species. Samples of γ_2-NiH+H_2 were compressed to 34, 40, and 52 GPa and laser heated at each pressure. Following laser heating at 40 GPa new peaks could be observed in the diffraction pattern; however, these new unexplained peaks disappeared on returning to ambient temperatures. At 52 GPa, *in situ* x-ray diffraction patterns show the disappearance of peaks due to γ_2-NiH, which were replaced by numerous new peaks that remained on quenching (Fig. 1). Heating was localized to the NiH sample and temperatures were estimated to be less than 1000 K as no blackbody radiation was detectable from the sample during heating. All the observed peaks could be uniquely indexed to a body-centered monoclinic unit cell $a = 6.1137(3)$, $b = 2.4701(1)$, $c = 6.4019(3)$ Å, and $\beta = 93.603(4)^\circ$ at 52 GPa [38]. Systematic absences were consistent with space groups without glide-plane symmetry elements and structure solution by charge flipping suggested space group $I2/m$ [39]. Despite extensive texturing of the diffraction rings, Rietveld refinement could be applied to several datasets giving reasonable agreement factors in this space group. Ni-atom positions and thermal parameters could be refined, with two Ni-atom sites (see Fig. 1 caption for atomic positions).

Likely H-atom positions were identified using an electrostatic potential map based on DFT calculations of the Ni-atom unit cell. A range of possible stoichiometries were generated by the stepwise placement of H atoms, giving compositions from Ni_2H to Ni_4H_9. Evaluating the relative enthalpies shows only a single stoichiometry, Ni_2H_3, to become more stable than a combination of NiH and excess Ni or H_2: above 54.8 GPa Ni_2H_3 is more stable than 2 NiH + $\frac{1}{2}H_2$; by 60 GPa the formation enthalpy is -11.6 meV/Ni_2H_3. The optimized structure from DFT calculations is shown in Fig. 2; unit-cell dimensions and structural parameters are given in Table I. There are two unique Ni-atom positions coordinated by eight and seven H atoms, respectively, forming irregular polyhedra. Direct comparison of Ni-H bond distances between γ_2-NiH at the same pressure shows that the synthesis of Ni_2H_3 leads to an increase in coordination number without a significant

TABLE I. Atomic position parameters refined by DFT for Ni_2H_3 at 55 GPa, $a = 6.110$, $b = 2.467$, $c = 6.416$ Å, $\beta = 93.37^\circ$, space group $I2/m$.

Atom	Site	x	y	z
Ni1	4*i*	0.71014	0	0.06893
Ni2	4*i*	0.07325	0	0.24375
H1	2*d*	0	0	$\frac{1}{2}$
H2	2*a*	0	0	0
H3	4*i*	0.61809	0	0.30373
H4	4*i*	0.30209	0	0.38897

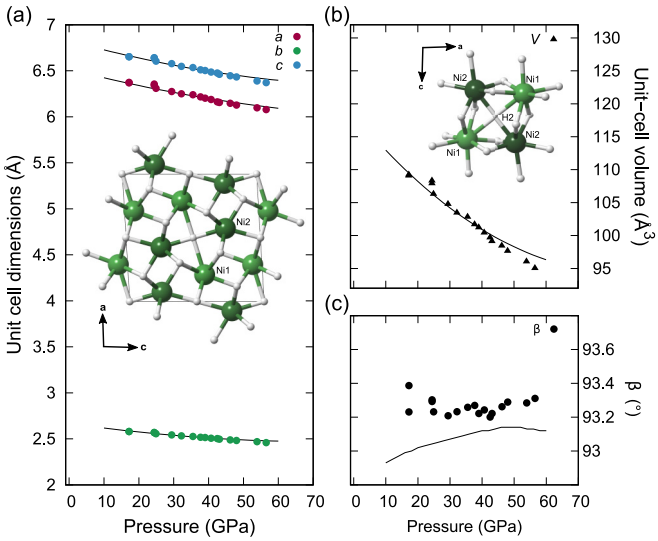

FIG. 2. (a) Ni_2H_3 unit-cell dimensions as a function of pressure. Inset: Crystal structure of Ni_2H_3 which crystallizes in space group $I2/m$ with two unique Ni atoms. (b) Ni_2H_3 unit-cell volume as a function of pressure. Inset: Ni_2H_3 structure showing four-coordinated H atoms in a distorted square planar arrangement. (c) Monoclinic angle, β, as a function of pressure. Data points in (a)–(c) are from experiments while lines correspond to values derived from DFT calculations at 0 K.

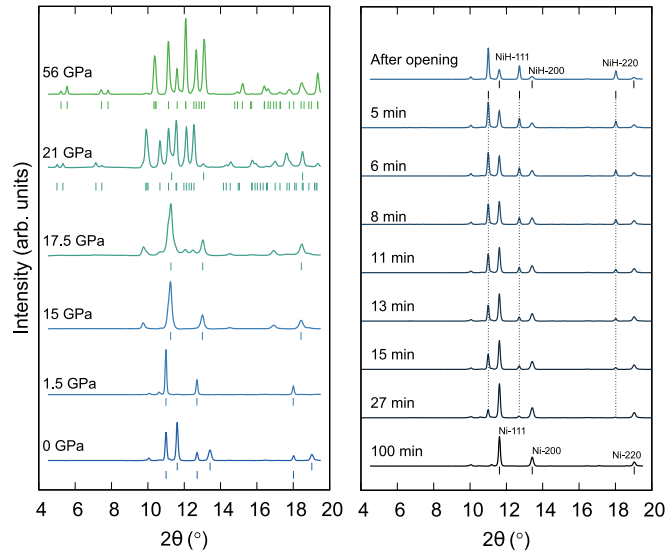

FIG. 3. High-pressure x-ray diffraction patterns ($\lambda = 0.4131$ Å) taken on decompression showing (left) the stepwise decomposition of Ni_2H_3 into γ_2-NiH and (right) the subsequent decomposition of γ_2-NiH into Ni and H_2 at ambient pressure.

decrease in Ni-H bond distances. The structure of Ni_2H_3 partially retains the Ni_4H_4 cubic units of γ_2-NiH but in distorted form, additional H atoms (H2) are coordinated by four Ni atoms forming distorted squares in the ac plane, breaking up the regular fcc lattice [inset, Fig. 2(b)]. The emergence of lower H-atom coordination has been predicted in several transition-metal hydrides and may lead to the formation of H-atom layers with increasing pressure and hydrogen content [11,40,41]. Over the stability range of Ni_2H_3 there is close agreement between the experimentally observed unit-cell dimensions and those derived from DFT calculations (Fig. 2), supporting our assignment of the hydrogen content. However, this should be experimentally verified by high-pressure neutron diffraction. The pressure-volume behaviors of NiH and Ni_2H_3 were fitted with third-order Birch-Murnaghan equations of state giving the parameters shown in Table II.

Magnetism was considered in the calculations for pure Ni, but not for the hydrides; a magnetic calculation of the γ_2-NiH rapidly demagnetized at all pressures. It is not clear whether this is an artifact of DFT preferring nonmagnetic solutions or if metal hydrides are inherently nonmagnetic. Note that recent structure predictions in a similar system, Cr-H, also exclusively find nonmagnetic hydrides [42]. Either way, this should not affect the stability of Ni_2H_3 against γ_2-NiH and H_2.

As can be seen in Fig. 3, on decompression below 25 GPa, weak peaks corresponding to γ_2-NiH begin to appear, and by 17.5 GPa, they fully replace those of Ni_2H_3. Reflections from γ_2-NiH could be observed down to ambient pressure and continue to remain upon opening the diamond-anvil cell to atmospheric conditions. Once quenched, we see the appearance of diffraction peaks corresponding to pure Ni and these reflections grow with time as the reflections from γ_2-NiH decrease in intensity. After approximately 1 h, no reflections due to γ_2-NiH could be observed leaving only those due to Ni (see Fig. 3).

The recovery of γ_2-NiH to low pressures (0.34 GPa) at room temperature, and recovery to ambient pressure at low temperatures (85 K) have been observed before [43–45]. The metastable preservation to ambient pressure at room temperature is unexpected and the reason for this is not fully understood. The transition from γ_1-NiH + H_2 to γ_2-NiH is known to be sluggish so it is likely that the transition from γ_2-NiH to Ni + H_2 is also kinetically hindered which resulted in the continued presence of the γ_2-NiH structure at ambient pressure [45]. As the hydrogen content of the structure cannot be directly determined from our x-ray diffraction data, future large-volume neutron diffraction experiments exploring the synthesis and quench are imperative toward the consideration of γ_2-NiH as a hydrogen storage medium.

In conclusion, we have explored the Ni-H system up to pressures of 60 GPa with combined x-ray diffraction and laser heating. With this method we have synthesized a Ni_2H_3 species by reaction of γ_2-NiH and H_2 at pressures above 50 GPa. Ni_2H_3 remains stable down to approximately 17 GPa

TABLE II. Birch-Murnaghan equation of state parameters for Ni [13], γ_2-NiH, and Ni_2H_3. B_0' was freely refined for both NiH and Ni_2H_3.

Phase	V_0 (Å^3/Z)	B_0 (GPa)	B_0'
Ni [13]	10.9315	181	5.2
γ_2-NiH (this work)	13.06(24)	191(10)	3.8(4)
γ_2-NiH [19]	13.14(2)	176(2)	4 (fixed)
Ni_2H_3	14.9(19)	204(43)	2.2(9)

before transforming to γ_2-NiH. At ambient temperatures γ_2-NiH can be quenched to atmospheric pressure whereupon it releases H_2 as it slowly transforms into pure Ni.

Note added. Recently, an independent study described the prediction and subsequent experimental observation of the same Ni_2H_3 compound [46]. Their reported synthesis pressure (60 GPa) is higher than in this study (52 GPa); however, the decomposition pressure, unit-cell dimensions, and derived equation of state parameters are in close agreement with our data [46].

The authors thank S. Imada-Kawaguchi and N. Hirao for their assistance during experiments. This work was performed under Proposal No. 2018A1041 at SPring-8.

[1] Y. Song, Phys. Chem. Chem. Phys. **15**, 14524 (2013).
[2] T. Bi, N. Zarifi, T. Terpstra, and E. Zurek, arXiv:1806.00163.
[3] A. P. Drozdov, M. I. Eremets, I. A. Troyan, V. Ksenofontov, and S. I. Shylin, Nature (London) **525**, 73 (2015).
[4] E. Wigner and H. B. Huntington, J. Chem. Phys. **3**, 764 (1935).
[5] N. W. Ashcroft, Phys. Rev. Lett. **21**, 1748 (1968).
[6] P. Dalladay-Simpson, R. T. Howie, and E. Gregoryanz, Nature (London) **529**, 63 (2016).
[7] X.-D. Liu, P. Dalladay-Simpson, R. T. Howie, B. Li, and E. Gregoryanz, Science **357**, eaan2286 (2017).
[8] A. E. Carlsson and N. W. Ashcroft, Phys. Rev. Lett. **50**, 1305 (1983).
[9] N. W. Ashcroft, Phys. Rev. Lett. **92**, 187002 (2004).
[10] M. Wang, J. Binns, M.-E. Donnelly, M. Peña-Alvarez, P. Dalladay-Simpson, and R. T. Howie, J. Chem. Phys. **148**, 144310 (2018).
[11] C. M. Pépin, G. Geneste, A. Dewaele, M. Mezouar, and P. Loubeyre, Science **357**, 382 (2017).
[12] A. Marizy, G. Geneste, P. Loubeyre, B. Guigue, and G. Garbarino, Phys. Rev. B **97**, 184103 (2018).
[13] P. Lazor, Ph.D. thesis, Uppsala University (1994).
[14] C. C. Yang, C. C. Wang, M. M. Li, and Q. Jiang, J. Mater. Chem. A **5**, 1145 (2017).
[15] V. E. Antonov, J. Alloys Compd. **330-332**, 110 (2002).
[16] Y. Fukai, S. Yamatomo, S. Harada, and M. Kanazawa, J. Alloys Compd. **372**, L4 (2004).
[17] E. O. Wollan, J. W. Cable, and W. C. Koehler, J. Phys. Chem. Solids **24**, 1141 (1963).
[18] V. Antonov, I. Belash, and E. Poniatovskii, Dokl. Akad. Nauk USSR **233**, 1114 (1977) [in Russian].
[19] N. Ishimatsu, T. Shichijo, Y. Matsushima, H. Maruyama, Y. Matsuura, T. Tsumuraya, T. Shishidou, T. Oguchi, N. Kawamura, M. Mizumaki, T. Matsuoka, and K. Takemura, Phys. Rev. B **86**, 104430 (2012).
[20] X. San, Y. Ma, T. Cui, W. He, B. Han, B. Liu, and G. Zou, Phys. Rev. B **74**, 052405 (2006).
[21] H. K. Mao, J. Xu, and P. M. Bell, J. Geophys. Res. **91**, 4673 (1986).
[22] Y. Fei, A. Ricolleau, M. Frank, K. Mibe, G. Shen, and V. Prakapenka, Proc. Natl. Acad. Sci. USA **104**, 9182 (2007).
[23] Y. Ohishi, N. Hirao, N. Sata, K. Hirose, and M. Takata, High Press. Res. **28**, 163 (2008).
[24] C. Prescher and V. B. Prakapenka, High Press. Res. **35**, 223 (2015).
[25] R. Oishi-Tomiyasu, J. Appl. Crystallogr. **47**, 593 (2014).
[26] A. Le Bail, H. Duroy, and J. Fourquet, Mater. Res. Bull. **23**, 447 (1988).
[27] H. M. Rietveld, J. Appl. Crystallogr. **2**, 65 (1969).
[28] V. Petříček, M. Dušek, and L. Palatinus, Z. Kristallogr. **229**, 345 (2014).
[29] G. Kresse and J. Furthmüller, Phys. Rev. B **54**, 11169 (1996).
[30] G. Kresse and D. Joubert, Phys. Rev. B **59**, 1758 (1999).
[31] J. Klimeš, D. R. Bowler, and A. Michaelides, J. Phys.: Condens. Matter **22**, 022201 (2010).
[32] J. Klimeš, D. R. Bowler, and A. Michaelides, Phys. Rev. B **83**, 195131 (2011).
[33] Y. Shizuku, S. Yamamoto, and Y. Fukai, J. Alloys Compd. **336**, 159 (2002).
[34] J. Schirber and B. Morosin, Phys. Rev. B **12**, 117 (1975).
[35] B. Li, Y. Ding, D. Y. Kim, R. Ahuja, G. Zou, and H.-K. Mao, Proc. Natl. Acad. Sci. USA **108**, 18618 (2011).
[36] E. Gregoryanz, C. Sanloup, M. Somayazulu, J. Badro, G. Fiquet, H.-k. Mao, and R. J. Hemley, Nat. Mater. **3**, 294 (2004).
[37] C. M. Pépin, A. Dewaele, G. Geneste, P. Loubeyre, and M. Mezouar, Phys. Rev. Lett. **113**, 265504 (2014).
[38] The standard C-centered cell can be obtained by application of the matrix $[(0, 0, 1)(0, 1, 0)(\bar{1}, 0, 1)]$.
[39] G. Oszlányi and A. Süto, Acta Crystallogr. A **60**, 134 (2004).
[40] P. Zaleski-Ejgierd, V. Labet, T. A. Strobel, R. Hoffmann, and N. W. Ashcroft, J. Phys.: Condens. Matter **24**, 155701 (2012).
[41] X. Feng, J. Zhang, H. Liu, K. Yin, and H. Wang, Solid State Commun. **239**, 14 (2016).
[42] S. Yu, X. Jia, G. Frapper, D. Li, A. R. Oganov, Q. Zeng, and L. Zhang, Sci. Rep. **5**, 17764 (2015).
[43] I. Czarnota and B. Baranowski, B. Pol. Acad. Sci. **14**, 191 (1966).
[44] G. Alefeld and J. Völkl, *Hydrogen in Metals II*, Topics in Applied Physics Vol. 29 (Springer-Verlag, Berlin/Heidelberg, 1978).
[45] V. E. Antonov, A. S. Ivanov, M. A. Kuzovnikov, and M. Tkacz, J. Alloys Compd. **580**, S109 (2013).
[46] J. Ying, H. Liu, E. Greenberg, V. B. Prakapenka, and V. V. Struzhkin, Phys. Rev. Mater. **2**, 085409 (2018).